Conformational stabilization of a β-hairpin through a triazole-tryptophan interaction

Donatella Diana[1], Claudia Di Salvo[1,2], Veronica Celentano[1], Lucia De Rosa[1], Alessandra Romanelli[3,4], Roberto Fattorusso[5], Luca D. D'Andrea[1*]

[1]Istituto di Biostrutture e Bioimmagini, CNR, Napoli, Italy

[2]present address: School of Chemistry, National University of Ireland Galway, Galway, Ireland

[3]Dipartimento di Farmacia, Università di Napoli "Federico II", Napoli, Italy

[4]present address: Dipartimento di Scienze Farmaceutiche, Università di Milano, Milano, Italy

[5]Dipartimento di Scienze e Tecnologie Ambientali, Biologiche e Farmaceutiche, Università della Campania "L. Vanvitelli", Caserta, Italy

*Corresponding author: [1]Istituto di Biostrutture e Bioimmagini, CNR, via Mezzocannone 16, 80134, Napoli, Italy; email: luca.dandrea@cnr.it

Keywords: click chemistry, β-hairpin, peptide, conformation, NMR, CuAAC, aromatic-aromatic interaction

Abstract

Molecular tools to stabilize β-hairpin conformation are needed as β-hairpin peptides are useful molecules for pharmaceutical, biological and material applications. We explored the use of a "triazole bridge", a covalent link between two β-hairpin strands obtained through Cu-catalyzed alkyne-azide cycloaddition, combined with an aromatic-aromatic interaction. High conformationally stable peptides were identified by NMR screening of a small collection of cyclic peptides based on the Trpzip2 scaffold. The characteristic Trp-Trp interaction of Trpzip2 was replaced by a diagonal triazole bridge of variable length. NMR and CD analyses showed that triazole and indole rings could favorable interact to stabilize a β-hairpin conformation. The conformational stabilization depends on the length of the triazole bridge and the reciprocal position between the aromatic rings. Combining aromatic interactions and the covalent inter-strands triazole bridge is an useful strategy to obtain peptides with high β-hairpin content.

Introduction

β-hairpin peptides are useful molecules for pharmaceutical and biomedical applications[1-3]. They are also attractive to modulate protein-protein interactions[4-8]. Stability and formation of β-hairpin have been deeply analyzed[9-14] and molecular tools have been developed to design conformationally stable β-hairpin peptides[9,15-18]. In the last years, we and others[19] have analyzed the conformational stability of β-hairpin peptides presenting a triazole bridge, with variable lengths, in a non-hydrogen bonded position (NHB)[20] and in a hydrogen bonded position (HB)[21]. The "triazole bridge" is a 1-4 disubstituted 1,2,3-triazole, obtained by side chain-side chain cyclization through Cu-catalyzed alkyne-azide cycloaddition (CuAAC),[22,23] forming a covalent linkage between β-hairpin strands. These previous studies have established that the formation of the inter-strands triazole bridge is an effective strategy to constrain peptides in a stable β-hairpin conformation and the optimal bridge length depends on the specific β-hairpin position (NHB or HB) of the tool[19-21]. However, we obtained peptides with a β-hairpin content lower than the tryptophan zipper 2 (Trpzip2)[17,24], a 12-mer peptide characterized by a cluster of cross-strands interactions between four tryptophan residues, which we refer as folded β-hairpin peptide.

Aromatic-aromatic interactions are important in stabilizing the structure of proteins[25,26], peptides[27-31] and in molecular recognition process[32,33]. In particular, aromatic interactions have been exploited to design stable β-hairpin peptides[6,17,34-36]. The 1,2,3-triazole is an aromatic heterocycle, nevertheless its role in establishing aromatic-aromatic interactions has never been explored for conformation stabilization purposes. We envisioned that if the triazole ring interacts with Trp, it will be possible to combine two stabilizing effects for a β-hairpin peptide: aromatic interactions and inter-strand covalent linkage.

In this work, we aim to obtain a high conformationally stable β-hairpin peptide combining aromatic-aromatic interactions and an inter-strand covalent linkage such as the triazole bridge. To

get this aim we designed a series of β-hairpin peptides presenting the triazole bridge in a diagonal non-hydrogen bonded (DNHB) position close to tryptophan side chain.

Results and discussion

Peptide Design and Synthesis. A set of nine peptides (Fig.1 and Fig.S1) was designed based on the Trpzip2 peptide, which presents a well-characterized β-hairpin structure and possesses an excellent thermodynamic stability[17]. Trpzip2 consists of a ENGK sequence, to promote a type I' turn, flanked by the tripeptide sequence WTW on both strands. The Trp residues are located in the NHB positions 2, 4, 9 and 11.

In our previous studies on the role of triazole bridge in NHB positions in β-hairpin peptides, we observed a weak NOE contact between Trp in position 2 and the cross-strand triazole bridge linking NHB positions 4 and 9, but we excluded any effect of triazole-tryptophan interaction on peptide stability[20]. In order to bring the two aromatic rings (triazole and indole) close and in a more favorable structural arrangement for interaction, we inserted the triazole bridge, with a diagonal arrangement, in the NHB positions 2 and 9 and leave the Trp in position 4 on the N-terminal strand. Previous works on diagonal non-covalent interactions showed that they can contribute to the stability of a β-hairpin peptide[37,38]. In analogy with our previous works, starting with Trpzip2 sequence, we replaced Trp11 with a Val residue and Trp2 and Trp9, respectively, with alkyne and azide amino acids having different side chain lengths to determine the optimal bridge length for the β-hairpin conformational stabilization. The schematic and complete sequences are reported in figure 1.

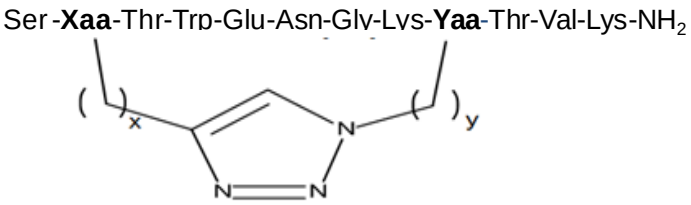

Peptide	Sequence[a]	x	y
Trpzip2	S-W-T-W-E-N-G-K-W-T-W-K-NH_2	-	-
DNHB 1.1	S-**Pra**-T-W-E-N-G-K-**Dap(N3)**-T-V-K-NH_2	1	1
DNHB 1.2	S-**Pra**-T-W-E-N-G-K-**Dab(N3)**-T-V-K-NH_2	1	2
DNHB 1.3	S-**Pra**-T-W-E-N-G-K-**Orn(N3)**-T-V-K-NH_2	1	3
DNHB 2.1	S-**Hpg**-T-W-E-N-G-K-**Dap(N3)**-T-V-K-NH_2	2	1
DNHB 2.2	S-**Hpg**-T-W-E-N-G-K-**Dab(N3)**-T-V-K-NH_2	2	2
DNHB 2.3	S-**Hpg**-T-W-E-N-G-K-**Orn(N3)**-T-V-K-NH_2	2	3
DNHB 3.1	S-**Bpg**-T-W-E-N-G-K-**Dap(N3)**-T-V-K-NH_2	3	1
DNHB 3.2	S-**Bpg**-T-W-E-N-G-K-**Dab(N3)**-T-V-K-NH_2	3	2
DNHB 3.3	S-**Bpg**-T-W-E-N-G-K-**Orn(N3)**-T-V-K-NH_2	3	3
DNHB 2.2rev	S-**Dab(N3)**-T-W-E-N-G-K-**Hpg**-T-V-K-NH_2	2	2
DNHB 2.2W3	S-**Hpg**-W-T-E-N-G-K-**Dab(N3)**-T-V-K-NH_2	2	2

Figure 1: Schematic representation and amino acid sequence of DNHB peptides. Xaa are alkyne amino acids: propargilglycine (Pra), homopropargilglycine (Hpg), bishomopropargilglycine (Bpg); Yaa are azide amino acids: L-β-azidoalanina (Dap(N3)), L-γ-azidohomoalanine (Dab(N3)), L-δ-azidoornitine (Orn(N3)).

Peptides were synthesized by Fmoc solid phase peptide synthesis. The alkyne amino acids propargilglycine (Pra), homopropargilglycine (Hpg), bishomopropargilglycine (Bpg) and the azido amino acids L-β-azidoalanina (Dap(N3)), L-γ-azidohomoalanine (Dab(N3)), L-δ-azidoornitine (Orn(N3)) were incorporated in the peptide sequence in different combinations. The purified peptides were subjected to an intramolecular CuAAC leading to the formation of a triazole bridge of different lengths (from two to six units) according to the number of methylene groups of the

alkyne and azido substituents (Fig. 1). As a proof of intramolecular cyclization by CuAAC and the occurred formation of 1,4 -disubstituted 1,2,3-triazole bridge we verified that: a) the linear peptides and the corresponding cyclized peptides have the same molecular mass but different HPLC elution times as already reported[20,39] (see Experimental section and figure S2 and S3); b) the absence of odd multi-charged peaks in the ESI-MS spectra suggesting the monomeric nature of the peptides (ESI-MS spectra of linear and cyclized peptides are reported in Figure S2 and S3); c) the cyclized peptides are stable to treatment with TCEP (as result of triazole formation), while linear peptides, in the same conditions, loss 26 Da as a consequence of the reduction of azide group to amine[20,40] (see Experimental section).

Circular dichroism analysis. In order to study the conformational properties of the synthesized peptides, circular dichroism (CD) spectroscopy analyses were performed in phosphate buffer at pH 6.6. CD spectra of linear DNHB peptides (Fig. S4) show an intense negative band at around 200 nm with a weak negative shoulder in the range 215-220 nm, suggesting that the linear peptides assume a predominantly unordered conformation in aqueous solution[41].

In contrast, cyclic DNHB peptides spectra show a negative band between 196 and 198 nm, less intense and blue-shifted of few nanometers with respect to the linear peptide, a negative band of variable intensity around 215 nm and a positive band at 227-229 nm is also present for few peptides (Fig. S5).

CD spectrum of a β-structure in the far-UV-region is characterized by a negative band around 217 nm and a positive band under 200 nm arising respectively from n-π* and π-π* transitions of the backbone amide groups. These bands could be masked, in peptide presenting aromatic residues, by π-π* transitions arising from interacting aromatic rings. This is the case of Trpzip peptides, whose CD spectra are dominated by exciton coupling between indole rings which produces a characteristic band splitting with a positive maximum at 225 and negative minimum at 218 nm[17,24]. β-hairpin peptides presenting interactions involving a Trp and an aromatic residue other than Trp have been

reported, for example Trp-Tyr, Trp-Phe[42-44]. Their CD spectra are characterized by multiple bands making unambiguous interpretation difficult. In general, a less intense positive band at 225 nm is observed, the negative band at 218 nm become a shoulder of a more intense negative band around 200 nm.

CD spectra analysis of cyclic DNHB peptides is not trivial as several factors can contribute to the spectra observed; in fact, the DNHB peptides differ for β-structure content, β-turn folding, strands twist imposed by the triazole bridge and strength of aromatic-aromatic interaction. However, we suppose that the anomalous far-UV spectra of cyclic DNHB peptides mainly reflect the interaction between the triazole and indole rings and the spectra diversity depends on the different geometry of interaction, which is dictated by the constrain imposed by the covalent cyclization through the triazole bridge. This hypothesis is supported by the CD spectra of DNHB2.2W3 peptide (Fig. S6). This peptide (sequence in figure 1) presents non-interacting aromatic rings as the triazole and the Trp side chain are on opposite sides of the β-hairpin. Its CD spectrum has a shape very similar to that of linear peptide with a minimum at 201 nm, a shoulder around 220 nm but no evident bands in the 215-220 nm region. DNHB2.2W3 peptide shows a low β-hairpin content, as determined by NMR (see next paragraph), but cyclic DNHB peptides with a similar β-hairpin content, for example DNHB1.1 or DNHB1.2, show a completely different CD spectrum (Fig. S5, left panel). These observations suggest that the CD spectrum of cyclic DNHB2.2W3 is indicative of a peptide with low β-hairpin content in absence of aromatic interactions (NMR analysis excluded any NOE contact between the two rings, see *infra*).

Evaluation of β-hairpin content by NMR spectroscopy. A combination of ^{1}H one-dimensional (1D) and bi-dimensional (2D) DQF-COSY, TOCSY, NOESY data sets were used to determine if DNHB peptides, both linear and cyclic, were folded into β-hairpin structures and to what extent they were folded.

The 1D ^{1}H NMR spectra of linear peptides showed amide chemical shift dispersions typical of unordered structures; after cyclization the peptides acquired a good chemical shift dispersion of the backbone amide protons, as occurs in a folded peptide (Fig. 2 and Fig. S7). Furthermore, the hairpin conformation for all cyclic peptides was confirmed by the splitting of the diastereotopic Hα atoms of the turn Gly7 residue (ΔδGly), as showed in Figure 2B.

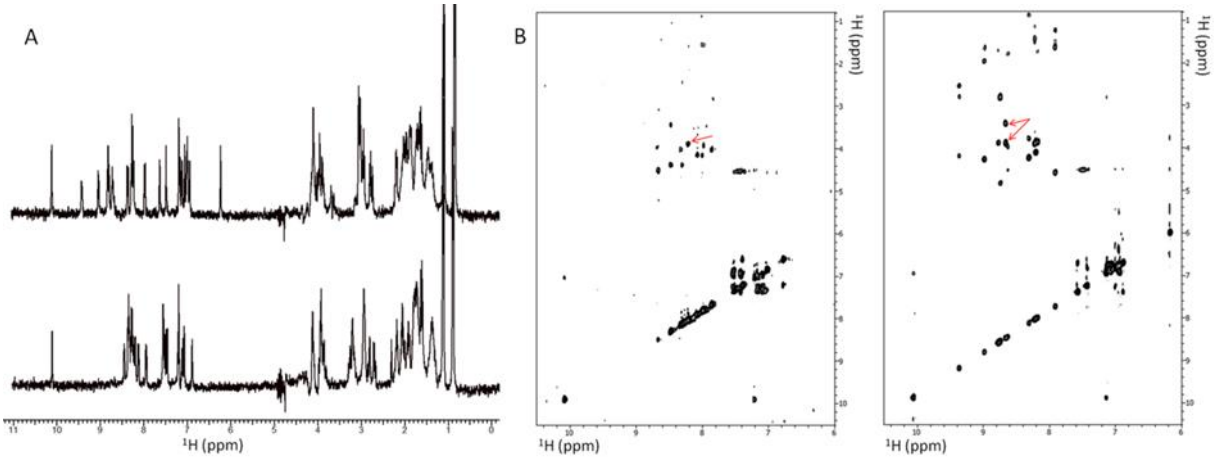

Figure 2: A) ^{1}H spectra of linear (lower) and cyclic (upper) DNHB 2.2 peptide in water solution. B) Section of the 2D [^{1}H, ^{1}H] TOCSY spectra of linear (left) and cyclic (right) DNHB 2.2 peptide. The arrows in the 2D [^{1}H, ^{1}H] TOCSY spectra highlight the Gly7 Hα protons. Spectra were recorded in water solution at 400 MHz and at 298 K.

The conformational properties of the cyclic peptides were qualitatively analyzed by comparing Hα chemical shifts relative to random coil values (ΔδHα)[45]. In particular, as shown in Figure 3, residues 2-4 and 9-11 show significant downfield shifts consistent with the pattern expected for an antiparallel β-sheet. Asn6, Gly7, Lys8 are upfield shifted as typically detected for residues in turn conformation while Ser1 and Lys12 are in a random coil conformation as usually observed at N- and C- termini.

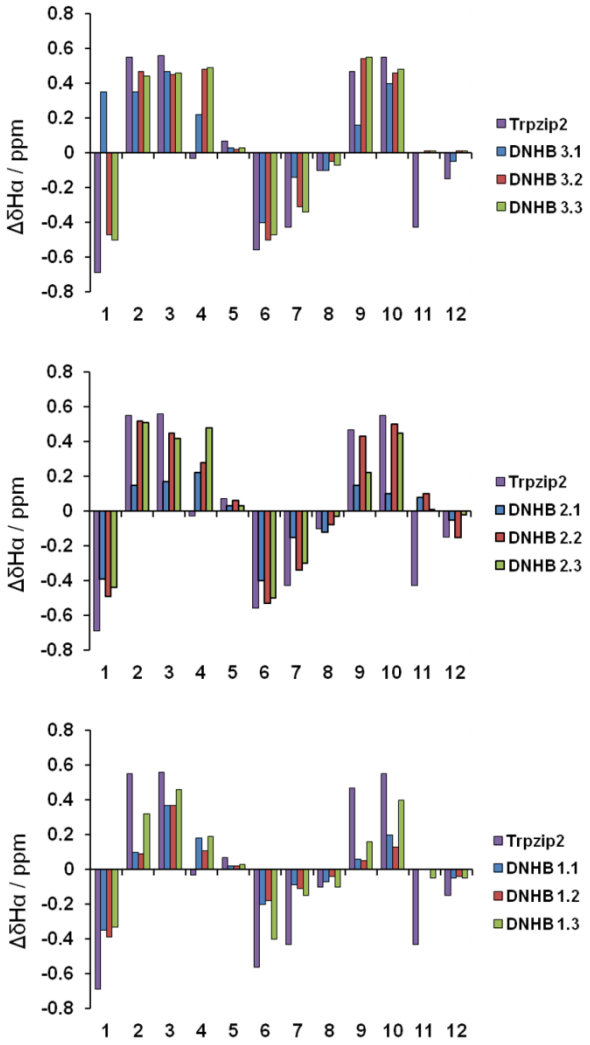

Figure 3: Hα chemical shift difference (ΔδHα) for Trpzip2 and for cyclic DNHB peptides.

Therefore, the extent of β-hairpin folding of each DNHB peptide was evaluated from different NMR parameters, the root mean square deviation of ΔδHα (RMSΔδHα) values taken for the residues located on the strands[14,20,21,46,47] and the ΔδGly in the turn of the hairpin[18,20,21,31,48]. The values determined for the DNHB peptides were compared to that obtained for Trpzip2, allowing us to rank DNHB peptides based on their conformational stability (Fig. 4 and Table S1). This analysis, a part from the validity of the two-state assumption, is limited by the absence of accurate reference values for the completely folded and random coil states which affects the precision and accuracy of the absolute quantification of β-sheet populations[49] but it is still effective to compare and rank a homogenous set of peptides. The two methods, which monitor different structural elements, are in a good agreement. A comparison of fraction-folded values derived from both Gly7 Hα splitting and

the RMSΔδHα reveals that the cyclic peptides retain a folded β-hairpin in the range of 31–96% with respect to Trpzip2 population.

Peptides with the number of methyl units inverted (1.2 vs 2.1, 1.3 vs 3.1, or 2.3 vs 3.2) show a similar β-hairpin content. Considering the azide component fixed and varying the alkynes on the N terminal strand, the β-hairpin content increases with the length of the side chain of the alkynes (DNHB1.1 < DNHB2.1 < DNHB3.1; DNHB1.2 < DNHB2.2 ≈ DNHB3.2; DNHB1.3 < DNHB2.3 < DNHB3.3). At the same way, fixed the alkyne component, the β-hairpin content increases with the length of the side chain of the azide (DNHB1.1 ≈ DNHB1.2 < DNHB1.3; DNHB2.1< DNHB2.3 < DNHB2.2; DNHB3.1< DNHB3.2 ≈ DNHB3.3). It seems that a minimum side chain length is required (peptides DNHB 2.2, 2.3, 3.2, and 3.3) to obtain high conformational stable β-hairpin peptide. For example, peptide DNHB2.2 assumes a high β-hairpin content (96% and 85% based on ΔδGly and RMSΔδHα respectively) with respect to Trpzip2 peptide. We can speculate that the minimum length of the triazole bridge is needed to confer a sufficient conformational flexibility to the triazole linkage to be accommodated into an adequate β-hairpin structure.

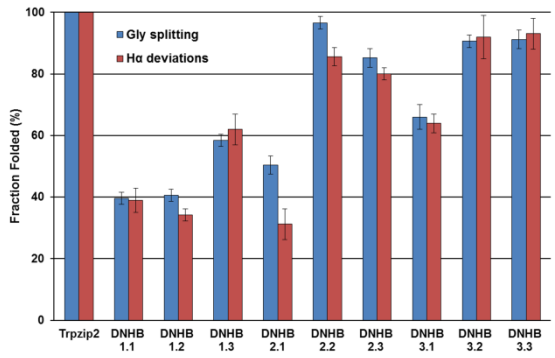

Figure 4: Fraction folded of DNHB peptides as determined by RMSΔδHα and ΔδGly Hα splitting values at 298 K, using limiting shift values derived from Trpzip2.

Conformational analysis of DNHB2.2 peptide. To gain molecular details on the conformation assumed by DNHB peptides, we decided to characterize DNHB 2.2 peptide, which present the shortest bridge length between the peptide with highest β-hairpin content. To this aim examination

of long-range NOEs between residues in antiparallel strands of the β-hairpin was performed. Several strong interstrand HN–HN and Hα–HN interactions (Table S2) are readily detected, confirming the correct registry for the β-hairpin. Additional week NOEs are seen between Hδ1, Hζ2 and Hη2 of the Trp4 indole ring and the Hζ proton of the 1,2,3-triazole moiety suggesting an aromatic–aromatic interaction (Fig. 5). Moreover, the 1,2,3-triazole Hζ proton is upfield shifted (7.28 ppm) with respect to the value measured for the reference 1,2,3 triazole moiety (7.90 ppm in DMSO, 7.55 ppm in water[20]). At the last, the temperature coefficients reveal that the backbone amide protons of residues Thr3, Glu5, Lys8, Thr10 and Lys12 are likely involved in hydrogen bonding, suggesting that the inter-strand hydrogen-bonding pattern of the hairpin is the same as in Trpzip2 (Table S3).

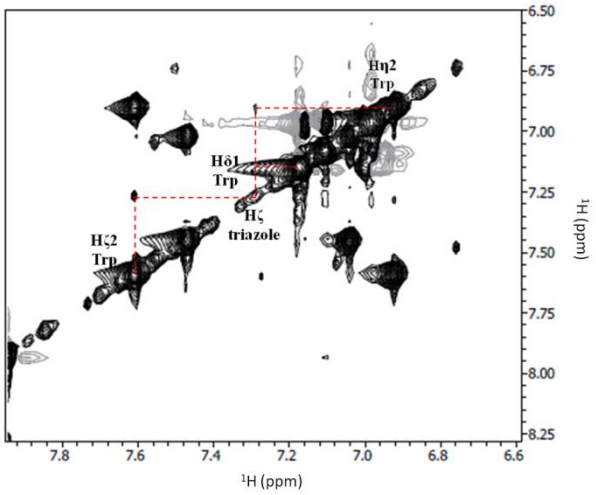

Figure 5: Aromatic region of the 2D NOESY spectrum of DNHB 2.2 cyclic peptide. Cross peaks between Hδ1, Hζ2 and Hη2 of Trp2 side chain and Hζ of 1,2,3 triazolyl moiety are highlighted.

Successively, we verified if hairpin stabilization of DNHB2.2 is strand-dependent synthesizing the peptide DNHB 2.2rev, where the alkyne and azide components are reversed. A comparison of the Hα shifts for DNHB2.2 and DNHB2.2rev showed a similar profile for both peptides (Fig. 6A). Indeed, the folded population of DNHB2.2rev was calculated to be 94% folded with glycine

splitting and 78% with RMSΔHα methods (Fig. 6B), indicating that no drastic change in hairpin folding occurs when the alkyne and azide components are exchanged.

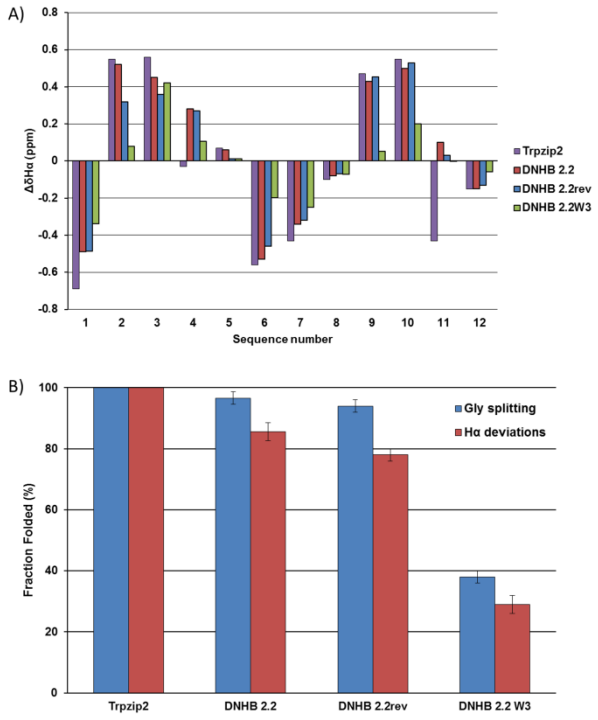

Figure 6: A) Hα chemical shift difference (ΔδHα) for Trpzip2 and for cyclic DNHB2.2, DNHB2.2rev and DNHB2.2W3 peptides. B) Fraction folded of DNHB2.2, DNHB2.2rev and DNHB2.2W3 peptides as determined by RMSΔδHα and ΔδGly Hα splitting values at 298 K, using limiting shift values derived from Trpzip2.

To investigate the influence of the aromatic interaction between the triazole moiety and the Trp4 indole on the DNHB2.2 β-hairpin conformation, we synthesized the DNHB2.2W3 peptide swapping Trp2 and Thr3 residues. In this way, the triazole ring and the Trp side chain fall on the two opposite side of the β-hairpin. This peptide showed considerably less Hα downfield shifting (Fig. 6A). Moreover, very few cross-strand interactions were detected for DNHB2.2W3 by NOESY experiments which suggests a poorly folded system (Table S4). In DNHB2.2W3 no NOE cross-peaks were detected between the 1,2,3-triazole and the indole ring, thus excluding aromatic interactions. The β-hairpin folded population for DNHB 2.2W3 was estimated to be 29% and of

38% with respect to Trpzip2 based on RMSΔHα and glycine splitting methods, respectively (Fig. 6B). The strong β-hairpin destabilization of DNHB2.2W3 and the NOEs between Trp4 indole protons ring and the Hζ proton of the 1,2,3-triazole ring detected in DNHB 2.2, strongly support the role of aromatic interaction between the triazole ring and the tryptophan side chain on the conformational stability of the β-hairpin peptide. It is well known that aromatic groups interact each other according specific geometric arrangements[33]; in particular aromatic amino acid residues interact using a T-shaped geometry with residues occupying a face or edge position. Upfield shifted resonance of a specific aromatic proton is indicative of an edge position[35,50]. In DNHB2.2 peptide, chemical shift of Trp aromatic protons are in random coil ranges indicating for this residue a face position; instead, triazole Hζ proton is upfield shifted therefore suggesting an edge-like position.

According with NMR analysis, the CD spectrum of cyclic DNHB2.2W3 in the far UV region shows a minimum around 200 nm with minor changes with respect to the linear peptide spectrum. This spectrum is different from the spectrum of DNHB2.2 peptide (Fig. 7A). Furthermore, we analyzed DNHB2.2 and DNHB2.2W3 peptides in the near UV region to analyze the CD spectra of aromatic chromophores (Fig. 7B). DNHB2.2W3 spectrum indicates the presence of an indole moiety completely exposed to the solvent as observed in L-Trp[51] or in the dipeptide Gly-Trp[52] in water which has been indicated as type 2 spectrum[53]. Instead, DNHB2.2 presents a type 3 spectrum with two negative minima at 281 and 288 nm as observed for *cyclo*(-His-Trp)[53] or Trp-Trp[52] in water suggesting that the indole is interacting with a close aromatic ring.

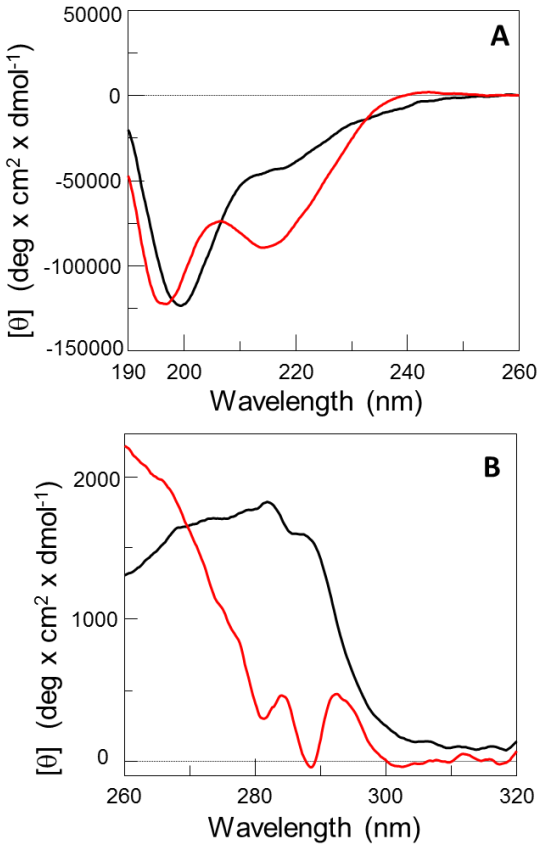

Figure 7: A) Far-UV circular dichroism spectra of cyclic DNHB2.2W3 (black line) and DNHB2.2 (red line) peptides in 10 mM phosphate buffer pH 6.6. B) Near-UV circular dichroism spectra of cyclic DNHB2.2W3 (black line) and DNHB2.2 (red line) peptides in 10 mM phosphate buffer pH 6.6. Spectra are reported in molar ellipticity ([θ]).

The strong destabilization of the β-hairpin structure observed in DNHB2.2W3 reveals that the triazole bridge (with x=y=2) in diagonal position is weakly stabilizing by itself. Similarly, the W2W9 peptide, a Trpzip2 analogue presenting only two tryptophan residues in a diagonal arrangement, mainly shows an unordered conformation[24]. In our previous study on the role of triazole bridge in NHB positions[20] the values of the ΔδGly splitting of the most stable peptide (NHB2.1) and its analogue with Trp flipped (NHB2.1W3) resulted comparable, therefore, suggesting that in the NHB peptide series the contribution of tryptophan side chain to the stabilization of the β-hairpin is irrelevant. This result highlights that in order to establish an efficient

interaction between the triazole bridge and the Trp, it is not sufficient that the two aromatic rings are on the same side of the hairpin but an optimal reciprocal position should be found. Finally, comparing the β-hairpin content of Trpzip2 and its analogue W2W4W9 with NHB2.1 and DNHB2.2 peptides (Fig. 8) we observed that the triazole bridge is less effective in replacing a cross-strand Trp pair (W2W4W9 vs NHB2.1) and more effective of a diagonal Trp-Trp interaction (W2W4W9 vs DNHB2.2). Furthermore, the formation of the triazole bridge covalently link the two β-strands and it is expected to improve the metabolic stability of the peptide[19,54].

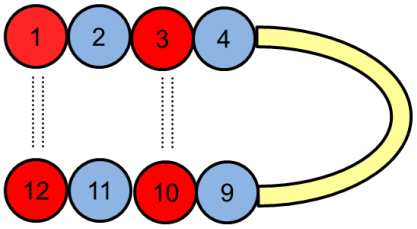

Peptide	Pattern				β-hairpin
Name	2	4	9	11	content
Trpzip2	W	W	W	W	1
W2W4W9	W	W	W	V	0.76[a]
NHB2.1	W	Hpg	Dap(N3)	V	0.60[a]
DNHB2.2	Hpg	W	Dab(N3)	V	0.97

Figure 8. Comparison between β-hairpin content of Trpzip and triazole bridged peptides. Top, schematic representation of studied β-hairpin peptides. Red and blue circles indicate hydrogen bonded and non-hydrogen bonded position. The yellow segment represent the four residues forming the β-turn. Bottom, correlation between Trp residues or triazole bridge position and peptide β-harpin content. [a]Value taken from Celentano et al. 2012[20]

Conclusion

The triazole bridge-Trp interaction is an useful strategy to design peptides with high β-hairpin content. In fact, triazole and indole rings favorable interact to stabilize a β-hairpin conformation.

The conformational stabilization depends on the length of the triazole bridge and the reciprocal position between the two aromatic rings. Combining aromatic interactions and the inter-strand triazole bridge covalent tool peptides with high β-hairpin content, similar to Trpzip2 peptide, have been obtained.

Experimental

Materials and methods

The Rink Amide MBHA resin (0.51 mmol/g), Fmoc-amino acids and activators such as HOBt and HBTU were provided by Novabiochem (Merck group, UK). Solvents for peptide synthesis and purification, acetic anhydride, ascorbic acid and copper sulfate (II) were purchased from Sigma-Aldrich (Italy). Alkyne and azide amino acids such as Fmoc-L-Dap (N3)-OH, Fmoc-L-Dab (N3)-OH, Fmoc-L-Orn (N3)-OH, Fmoc-Pra-OH, Fmoc-Hpg-OH, Fmoc-Bpg-OH were from Iris Biotech GmbH (Germany) or Chiralix B. V. (The Netherlands). N,N-diisopropylethylamine (DIPEA) was purchased from Sigma-Aldrich (Italy), while the piperidine was provided by the company Biosolve (France). Products purification were carried out by liquid chromatography in reverse phase high pressure (RP-HPLC) using an Agilent 1200 equipped with a diode array detector. Peptides analysis were performed on the instrument LC-MS LCQ Deca XP MAX (Thermo Fisher Scientific, Massachusetts, U.S.) equipped with an ESI source and an ion trap mass analyzer coupled to a surveyor HPLC system. The reversed phase column were from Phenomenex (Torrance, USA).

Peptide synthesis

The synthesis of all peptides was performed in manual solid phase using Fmoc chemistry on Rink-amide MBHA resin. After swelling of the resin in dimethylformamide (DMF) for about 30 minutes, Fmoc removal was effected by treating the resin with a basic solution constituted by 30% piperidine in DMF, twice for 5 minutes. The amino acids (2.5 equivalents) were coupled using solutions of HBTU/HOBt 0.45M (2.49 equivalents) in DMF, in the presence of DIPEA (5 equivalents). Double

couplings were performed 20 minutes at room temperature. The acetylation was carried out using a solution of acetic anhydride (2 M), DIPEA (0.55 M) and HOBt (0.06 M) dissolved in DMF for 5 minutes. At the end of the synthesis, the resin was washed with DMF, DCM, diethyl ether and dried under vacuum. The peptides were detached from the resin and deprotected by a treatment with a solution of TFA/TIS/H_2O (95:2.5:2.5, v/v/v) for three hours at room temperature. The crude peptides were precipitated in cold diethyl ether, collected after centrifugation, suspended in a solution of water/acetonitrile and lyophilized. The linear peptides were purified by preparative RP-HPLC using a AXIA column (50 x 21.2 mm, 4 μ) at a flow rate of 20 mL/min. The linear peptides were characterized by LC-MS using a C12 proteo column (50x2.0 mm, 4 μm). Peptides analysis was performed on a RP-HPLC using a Proteo C12 column (4 μm, 90 Å, 250 x 4.60 mm) and a linear gradient of H_2O (0.1% TFA)/CH_3CN (0.1% TFA) from 5% to 70% of CH_3CN in 20 min.

Analytical characterization of linear DNHB peptides:

DNHB1.1: MS(m/z) $[M+H]^+$calcd 1355.5, $[M+2H]^{2+}$calcd 678.2, found 678.7; RP-HPLC t_R=14.07 min

DNHB1.2: MS(m/z) $[M+H]^+$calcd 1369.6, $[M+2H]^{2+}$calcd 685.3, found 685.3; RP-HPLC t_R=14.25 min

DNHB1.3: MS(m/z) $[M+H]^+$calcd 1383.6, $[M+2H]^{2+}$calcd 692.3, found 692.4; RP-HPLC t_R=14.56 min

DNHB2.1: MS(m/z) $[M+H]^+$calcd 1369.6, $[M+2H]^{2+}$calcd 685.2, found 685.4; RP-HPLC t_R=14.22 min

DNHB2.2: MS(m/z) $[M+H]^+$calcd 1383.5, $[M+2H]^{2+}$calcd 692.3, found 692.3; RP-HPLC t_R=14.55 min

DNHB2.3: MS(m/z) $[M+H]^+$calcd 1397.6, $[M+2H]^{2+}$calcd 699.3, found 699.4; RP-HPLC t_R=14.85 min

DNHB3.1: MS(m/z) $[M+H]^+$calcd 1383.5, $[M+2H]^{2+}$calcd 692.2, found 692.6; RP-HPLC t_R=14.37 min

DNHB3.2: MS(m/z) $[M+H]^+$calcd 1397.6, $[M+2H]^{2+}$calcd 699.3, found 699.5; RP-HPLC t_R=14.55 min

DNHB3.3: MS(m/z) $[M+H]^+$calcd 1411.6, $[M+2H]^{2+}$calcd 706.3, found 706.2; RP-HPLC t_R=14.94 min

DNHB2.2rev: MS(m/z) $[M+H]^+$ calcd 1383.5, $[M+2H]^{2+}$calcd 692.3, found 692.6; RP-HPLC t_R=14.21 min

DNHB2.2W3: MS(m/z) $[M+H]^+$calcd 1383.5, $[M+2H]^{2+}$calcd 692.3, found 692.6; RP-HPLC t_R=14.17 min

Cu-catalyzed alkyne-azide cycloaddition

The purified linear peptides (0.5mM) dissolved in H_2O/CH_3OH (2:1 v/v) were cyclized using $CuSO_4$ (14 eq) and ascorbic acid (13 eq), the mixture was degassed with a gentle flow of N_2 for 5 min and then was stirred at room temperature for 1 h. Crude peptides were purified by RP-HPLC on a C12 proteo column (250x10.00 mm, 10 μm; flow = 5mL/min), the fractions were pooled and lyophilized. Clicked peptides purity were verified by analytical RP-HPLC using the specified gradient of CH_3CN (0.1% TFA) in H_2O (0.1% TFA) from 5% to 70% in 20 min. The purified cyclic peptides were characterized by LC-MS using a C12 proteo column (50x4.6mm, 4μm).

DNHB 1.1: MS (m/z) $[M+H]^{2+}$ calcd 1355.5, $[M+2H]^{2+}$ calcd 678.2, found 678.4; RP-HPLC t_R=12.44 min

DNHB 1.2: MS(m/z) $[M+H]^+$ calcd 1369.6, $[M+2H]^{2+}$ calcd 685.3, found 685.3; RP-HPLC t_R=12.55 min

DNHB 1.3: MS(m/z) $[M+H]^+$ calcd 1383.6, $[M+2H]^{2+}$ calcd 692.3, found 692.4; RP-HPLC t_R=12.79 min

DNHB 2.1: MS(m/z) $[M+H]^+$ calcd 1369.6, $[M+2H]^{2+}$ calcd 685.2, found 685.4; RP-HPLC t_R=12.62 min

DNHB 2.2: MS(m/z) $[M+H]^+$ calcd 1383.5, $[M+2H]^{2+}$ calcd 692.3, found 692.4; RP-HPLC t_R=12.66 min

DNHB 2.3: MS (m/z) $[M+H]^+$ calcd 1397.6, $[M+2H]^{2+}$ calcd 699.3, found 699.4; RP-HPLC t_R=12.92 min

DNHB 3.1: MS(m/z) $[M+H]^+$ calcd 1383.5, $[M+2H]^{2+}$calcd 692.2, found 692.5; RP-HPLC t_R=12.85 min

DNHB 3.2: MS(m/z) $[M+H]^+$ calcd 1397.6, $[M+2H]^{2+}$calcd 699.3, found 699.3; RP-HPLC t_R=12.84 min

DNHB 3.3: MS(m/z) $[M+H]^+$ calcd 1411.6, $[M+2H]^{2+}$calcd 706.3, found 706.4; RP-HPLC t_R=13.17 min

DNHB 2.2rev: MS(m/z) $[M+H]^+$ calcd 1383.5, $[M+2H]^{2+}$calcd 692.3, found 692.5; RP-HPLC t_R=12.8 min

DNHB 2.2W3: MS(m/z) $[M+H]^+$ calcd 1383.5, $[M+2H]^{2+}$calcd 692.3, found 692.5; RP-HPLC t_R=13.32 min

Reduction reaction

Reduction reactions were carried out using the reducing agent tris (2-carboxyethyl) phosphine (TCEP) solubilized in a Tris HCl buffer (50 mM), pH 7.5. The reducing solution was added to the cyclized purified peptides and to pure linear peptide DNHB 3.3, used as a reference of the reduction occurred. The reaction was left under stirring overnight. Analysis of the crudes was performed by ESI mass spectrometry using a Jupiter C18 column (5 μ, 300 Å, 250 x 2.0 mm) and a linear gradient of CH_3CN (0.05% TFA) in H_2O (0.05% TFA) from 5% to 70% in 20 minutes.

DNHB 1.1: MS (m/z) $[M+H]^{2+}$ calcd 1355.5, $[M+2H]^{2+}$ calcd 678.2, found 678.4;

DNHB 1.2: MS (m/z) $[M+H]^+$ calcd 1369.6, $[M+2H]^{2+}$ calcd 685.3, found 685.5;

DNHB 1.3: MS (m/z) $[M+H]^+$ calcd 1383.6, $[M+2H]^{2+}$ calcd 692.3, found 692.5

DNHB 2.1: MS (m/z) $[M+H]^+$ calcd 1369.6, $[M+2H]^{2+}$ calcd 685.2, found 685.5;

DNHB 2.2: MS (m/z) $[M+H]^+$ calcd 1383.5, $[M+2H]^{2+}$ calcd 692.3, found 692.5

DNHB 2.3: MS (m/z) $[M+H]^+$ calcd 1397.6, $[M+2H]^{2+}$ calcd 699.3, found 699.4

DNHB 3.1: MS (m/z) $[M+H]^+$ calcd 1383.5, $[M+2H]^{2+}$ calcd 692.2, found 692.5;

DNHB 3.2: MS (m/z) $[M+H]^+$ calcd 1397.6, $[M+2H]^{2+}$ calcd 699.3, found 699.5;

DNHB 3.3: MS (m/z) $[M+H]^+$ calcd 1411.6, $[M+2H]^{2+}$ calcd 706.5, found 706.3;

DNHB 3.3 lin red: MS (m/z) $[M+H]^+$ calcd 1385.6, $[M+2H]^{2+}$ calcd 693.3, found 693.5.

CD spectroscopy

The far-UV circular dichroism spectra were recorded using the J-810 spectropolarimeter (Jasco, Easton, US) equipped with a thermoregulation system Peltier PTC-423S/15, using quartz cells of 0.1 cm (Hellma , Milan, Italy). The peptides were solubilized in phosphate buffer (10 mM) pH 6.6 at a concentration of 50 μM. Circular dichroism spectra were recorded at 20 °C using a 260–190 nm measurement range, 10 nm/min scanning speed, 2 nm bandwidth, 4 s response time, 0.2 nm data pitch. Near-UV CD spectra were collected on a Jasco 720 (Easton, MD, US) spectropolarimeter, in the wavelength range 260-340 nm, using a 1 cm path-length quartz cuvette (Hellma, Milan, Italy) filled with 1.9 mL of peptide solutions. Spectra were collected at 20 °C, setting the following parameters: scanning speed 10 nm/min, bandwidth 2.0 nm, data pitch 0.2 nm, response 4 s, standard sensitivity and three spectra accumulations. Aliquots of the lyophilized peptides were dissolved in 10 mM potassium phosphate buffer pH 6.6 and centrifuged at 13200 rpm for 3 minutes, at room temperature. Supernatants were recovered, diluted to 1.9 mL with buffer and analyzed by CD.

Peptide concentrations were determined by evaluating the absorbance at 280 nm using a molar extinction coefficient of 5500 M^{-1} cm^{-1}. CD spectra are displayed in molar ellipticity. The processing of the spectra was obtained by using the Spectra Manager software (Jasco corporation, ver. 1.53.01). Spectra have been smoothed for clarity.

NMR spectroscopy

NMR samples were prepared dissolving the lyophilized peptides in $H_2O/^2H_2O$ (9:1 v/ v) at final concentrations ranging from 0.5 to 1.0 mM. The sodium 2,2-dimethyl-2-silapentane-5-sufonate (DSS) has been used as an internal reference. All NMR spectra were acquired on a Varian INOVA 400 Hz spectrometer. The suppression of the water signal was obtained through sequences Double Pulsed Field Gradient Spin Echo[55]. All spectra were processed with a software Sparky (Goddard, TD & Kneller, DG. SPARKY3, 2001) and analyzed with Neasy supported by a computer-aided resonance assignment (CARA) software[56]. The fraction folded was determined using the splitting Ha of glycine 7 in the turn by the equation: $(\Delta\delta Gly_{obs})/(\Delta\delta Gly_{100})$ where $\Delta\delta Gly_{obs}$ is the difference between the value of proton chemical shifts of glycine in the peptide cyclized and ΔδGly100 is the value of the proton chemical shifts of Glycine in Trpzip2. Moreover, simultaneously, an RMSD value taken over all residues (RMSΔδHα) as a measure of β-strand stability at a given temperature was calculated. The ratio $RMS\Delta\delta H\alpha / RMS\Delta\delta H\alpha_{limit}$ where the $RMS\Delta\delta H\alpha_{limit}$ is the Trpzip2 value, was used to calculate the β-hairpin fraction folded.

Acknowledgement

We would like to thank Mr L. Zona for technical assistance. D.D. was supported by the grant FIRB RBFR12WB3W 002 by MIUR. LDD thanks MIUR for support (PON03PE_00060_7).

References

(1) Yu, Z.; Cai, Z.; Chen, Q.; Liu, M.; Ye, L.; Ren, J.; Liao, W.; Liu, S. *Biomater Sci* **2016**, *4*, 365.

(2) Robinson, J. A.; Demarco, S.; Gombert, F.; Moehle, K.; Obrecht, D. *Drug Discov Today* **2008**, *13*, 944.

(3) Luther, A.; Moehle, K.; Chevalier, E.; Dale, G.; Obrecht, D. *Curr Opin Chem Biol* **2017**, *38*, 45.

(4) Wojcik, P.; Berlicki, L. *Bioorg Med Chem Lett* **2016**, *26*, 707.

(5) De Rosa, L.; Diana, D.; Basile, A.; Russomanno, A.; Isernia, C.; Turco, M. C.; Fattorusso, R.; D'Andrea, L. D. *Eur J Med Chem* **2014**, *73*, 210.

(6) Diana, D.; Basile, A.; De Rosa, L.; Di Stasi, R.; Auriemma, S.; Arra, C.; Pedone, C.; Turco, M. C.; Fattorusso, R.; D'Andrea, L. D. *J Biol Chem* **2011**, *286*, 41680.

(7) Fasan, R.; Dias, R. L. A.; Moehle, K.; Zerbe, O.; Obrecht, D.; Mittl, P. R. E.; Grutter, M. G.; Robinson, J. A. *Chembiochem* **2006**, *7*, 515.

(8) Robinson, J. A. *Acc Chem Res* **2008**, *41*, 1278.

(9) Ramirez-Alvarado, M.; Kortemme, T.; Blanco, F. J.; Serrano, L. *Bioorgan Med Chem* **1999**, *7*, 93.

(10) Maynard, A. J.; Sharman, G. J.; Searle, M. S. *J Am Chem Soc* **1998**, *120*, 1996.

(11) Dinner, A. R.; Lazaridis, T.; Karplus, M. *Proc Natl Acad Sci U S A* **1999**, *96*, 9068.

(12) Blanco, F.; Ramirez-Alvarado, M.; Serrano, L. *Curr Opin Struct Biol* **1998**, *8*, 107.

(13) Dyer, R. B.; Maness, S. J.; Peterson, E. S.; Franzen, S.; Fesinmeyer, R. M.; Andersen, N. H. *Biochemistry* **2004**, *43*, 11560.

(14) Griffiths-Jones, S. R.; Maynard, A. J.; Searle, M. S. *J Mol Biol* **1999**, *292*, 1051.

(15) Gellman, S. H. *Curr Opin Chem Biol* **1998**, *2*, 717.

(16) Kier, B. L.; Shu, I.; Eidenschink, L. A.; Andersen, N. H. *Proc Natl Acad Sci U S A* **2010**, *107*, 10466.

(17) Cochran, A. G.; Skelton, N. J.; Starovasnik, M. A. *Proc Natl Acad Sci U S A* **2001**, *98*, 5578.

(18) Hughes, R. M.; Waters, M. L. *J Am Chem Soc* **2005**, *127*, 6518.

(19) Park, J. H.; Waters, M. L. *Org Biomol Chem* **2013**, *11*, 69.

(20) Celentano, V.; Diana, D.; De Rosa, L.; Romanelli, A.; Fattorusso, R.; D'Andrea, L. D. *Chem Commun* **2012**, *48*, 762.

(21) Celentano, V.; Diana, D.; Di Salvo, C.; De Rosa, L.; Romanelli, A.; Fattorusso, R.; D'Andrea, L. D. *Chem-Eur J* **2016**, *22*, 5534.

(22) Tornøe, C. W.; Christensen, C.; Meldal, M. *J Org Chem* **2002**, *67*, 3057.

(23) Rostovtsev, V. V.; Green, L. G.; Fokin, V. V.; Sharpless, K. B. *Angew Chem Int Edit* **2002**, *41*, 2596.

(24) Wu, L.; McElheny, D.; Huang, R.; Keiderling, T. A. *Biochemistry* **2009**, *48*, 10362.

(25) Burley, S. K.; Petsko, G. A. *Trends Biotechnol* **1989**, *7*, 354.

(26) Serrano, L.; Bycroft, M.; Fersht, A. R. *J Mol Biol* **1991**, *218*, 465.

(27) Waters, M. L. *Biopolymers* **2004**, *76*, 435.

(28) Diana, D.; De Rosa, L.; Palmieri, M.; Russomanno, A.; Russo, L.; La Rosa, C.; Milardi, D.; Colombo, G.; D'Andrea, L. D.; Fattorusso, R. *Sci Rep* **2015**, *5*.

(29) Aravinda, S.; Shamala, N.; Rajkishore, R.; Gopi, H. N.; Balaram, P. *Angew Chem Int Edit* **2002**, *41*, 3863.

(30) Martin-Gago, P.; Gomez-Caminals, M.; Ramon, R.; Verdaguer, X.; Martin-Malpartida, P.; Aragon, E.; Fernandez-Carneado, J.; Ponsati, B.; Lopez-Ruiz, P.; Cortes, M. A.; Colas, B.; Macias, M. J.; Riera, A. *Angew Chem Int Edit* **2012**, *51*, 1820.

(31) Tatko, C. D.; Waters, M. L. *J Am Chem Soc* **2002**, *124*, 9372.

(32) Meyer, E. A.; Castellano, R. K.; Diederich, F. *Angew Chem Int Edit* **2003**, *42*, 1210.

(33) Salonen, L. M.; Ellermann, M.; Diederich, F. *Angew Chem Int Edit* **2011**, *50*, 4808.

(34) Espinosa, J. F.; Gellman, S. H. *Angew Chem Int Edit* **2000**, *39*, 2330.

(35) Santiveri, C. M.; Jimenez, M. A. *Biopolymers* **2010**, *94*, 779.

(36) Blanco, F. J.; Rivas, G.; Serrano, L. *Nat Struct Biol* **1994**, *1*, 584.

(37) Syud, F. A.; Stanger, H. E.; Gellman, S. H. *J Am Chem Soc* **2001**, *123*, 8667.

(38) Tatko, C. D.; Waters, M. L. *Protein Sci* **2003**, *12*, 2443.

(39) Jagasia, R.; Holub, J. M.; Bollinger, M.; Kirshenbaum, K.; Finn, M. G. *J Org Chem* **2009**, *74*, 2964.

(40) Punna, S.; Kuzelka, J.; Wang, Q.; Finn, M. G. *Angew Chem Int Edit* **2005**, *44*, 2215.

(41) Toniolo, C.; Formaggio, F.; Woody, R. W. In *Comprehensive Chiroptical Spectroscopy - Applications in Stereochemical Analysis of Synthetic Compounds, Natural Products, and Biomolecules*; Berova, N., Polavarapu, P. L., Nakanishi, K., Woody, R. W., Eds.; John Wiley & Sons, Inc: New York, 2012; Vol. 2, p 499.

(42) Mahalakshmi, R.; Shanmugam, G.; Polavarapu, P. L.; Balaram, P. *Chembiochem* **2005**, *6*, 2152.

(43) Mahalakshmi, R.; Raghothama, S.; Balaram, P. *J Am Chem Soc* **2006**, *128*, 1125.

(44) Makwana, K. M.; Mahalakshmi, R. *Chembiochem* **2014**, *15*, 2357.

(45) Wishart, D. S.; Sykes, B. D.; Richards, F. M. *J Mol Biol* **1991**, *222*, 311.

(46) Griffiths-Jones, S. R.; Searle, M. S. *J Am Chem Soc* **2000**, *122*, 8350.

(47) Fesinmeyer, R. M.; Hudson, F. M.; Olsen, K. A.; White, G. W. N.; Euser, A.; Andersen, N. H. *J Biomol NMR* **2005**, *33*, 213.

(48) Dyer, R. B.; Maness, S. J.; Franzen, S.; Fesinmeyer, R. M.; Olsen, K. A.; Andersen, N. H. *Biochemistry* **2005**, *44*, 10406.

(49) Pantoja-Uceda, D.; Santiveri, C. M.; Jimenez, M. A. *Methods Mol Biol* **2006**, *340*, 27.

(50) Makwana, K. M.; Mahalakshmi, R. *Chem-Eur J* **2016**, *22*, 4147.

(51) Strickland, E. H.; Horwitz, J.; Billups, C. *Biochemistry* **1969**, *8*, 3205.

(52) Edelhoch, H.; Lippoldt, R. E.; Wilchek, M. *J Biol Chem* **1968**, *243*, 4799.

(53) Strickland, E. H. *CRC Crit Rev Biochem* **1974**, *2*, 113.

(54) Meldal, M.; Tornøe, C. W. *Chem. Rev.* **2008**, *108*, 2952.

(55) Hwang, T. L.; Shaka, A. J. *J Magn Reson Ser A* **1995**, *112*, 275.

(56) Masse, J. E.; Keller, R. *J Magn Reson* **2005**, *174*, 133.

Graphical abstract

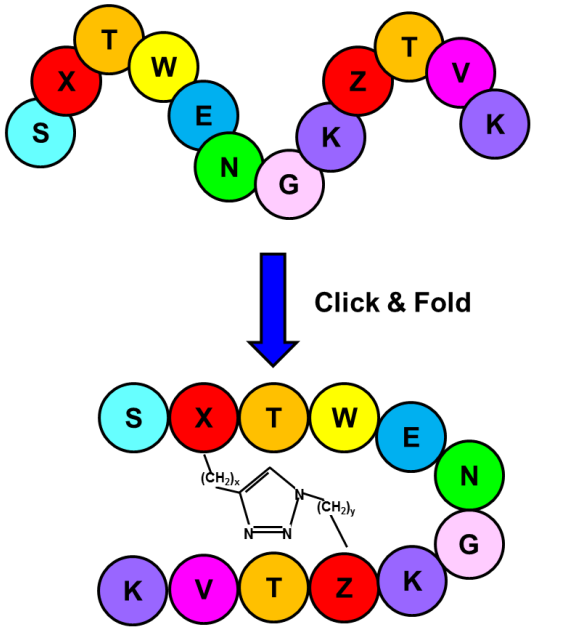

X= alkyne amino acids Z= Azide amino acids